

MULTI-RECOGNITION COMBINED SECURITY SYSTEM FOR INTELLIGENT CAR ELECTRONICS

GWO-JIA JONG, PENG-LIANG PENG AND GWO-JIUN HORNG

Department of Electronic Engineering
National Kaohsiung University of Applied Sciences
No. 415, Chien Kung Road, Sanmin District, Kaohsiung 80778, Taiwan
gjjong@cc.kuas.edu.tw

Received January 2011; revised May 2011

ABSTRACT. *This paper presents car electronics for a multi-recognition wireless communication and security system integrating radio frequency identification (RFID) and face recognition technology. The system combines the different advantages of RFID and face recognition technology. This car electronic system is optimal for an innovative specific application. Not only can the system protect the car, but it can determine responsibility in a car accident. Furthermore, the car electronic system integrates RFID, face recognition, general packet radio service (GPRS), Bluetooth and the global positioning system (GPS). It has been trending the merger goal of digitization. Therefore, it creates a tremendous amount of commercial opportunity.*

Keywords: Car electronics, RFID, Face recognition, GPRS

1. Introduction. Every year in the United States, about six million traffic accidents occur due to automobile crashes. In 2003 alone, these accidents accounted for \$230 billion in damaged property, 2,889,000 nonfatal injuries, and 42,643 deaths. The potential benefits of intelligent transportation system (ITS) car electronics include driving safety, transport efficiency and comfort, which arise from increased traffic information, reduced driving loads and improved route management [1,2].

More recently, the availability of the global positioning system (GPS) and the deployment of cellular-based communication systems have further fueled the development of vehicle tracking systems and systems to provide information to travelers in vehicles through wireless means [1]. Other technologies that facilitate intelligent transportation include vehicular telematics, vehicular radars and RFID. Among various applications, these technologies enable mayday systems, stolen-vehicle tracking, automatic route guidance and travel information, intelligent near-collision avoidance, tire-pressure monitoring, vehicle entry and security systems, electronic toll collection, automatic vehicle identification, and real-time location systems [2]. Implementation fields can be adopted for purchasing gas, going through tolls, paying for parking, checking security or troubleshooting engine problems, among other functions [3,4].

Traffic information collection is the foundation of traffic management, and accurate, detailed and timely data will guarantee the validity and credibility of the traffic supervision and control. According to an analysis of traffic control strategies, regardless of what type of strategy it is, it must receive ample information from the data collection system to exert its functions [5]. Compared with traditional loop detectors and GPS-based methods, this newly emerging approach has the benefits of low costs in device installation and maintenance, convenience in data collection and relatively large sample sizes, especially in peak hours [6].

This work contributes to research literature in three major areas: (1) In vehicle electronics environment, we consider a multiple secure mechanism that includes RFID technique and human recognition technique in order to upgrade the security efficiency; (2) This work transmits real time vehicle electronics information and warning information through GPRS technique; (3) We propose a mechanism that can monitor driver's behavior and vehicle electronics condition. Furthermore, we also detailedly record any kind of vehicle's information in the black box.

2. System Model. The immediate impacts of this system include alleviating vehicle-traffic congestion and improving operations management in support of public safety goals, such as collision avoidance. Our proposed scheme aims at supporting quality of service (QoS) for timely delivery of real-time data (e.g., car electronic safety messages and platoon commands) and for increasing the throughput for non-real-time data (e.g., RFID devices and face recognition).

The multi-recognition car electronic system is a major configuration that uses RFID and face recognition. It is implemented with the serial port transmitting data received from the server end by GPRS. The driver's identity is needed for confirmation at the server end, and the approved information is sent back to the client end. The car black box synchronously transmits data to the server end. The server end can back up the data every five minutes. The GPS receiver is embedded and communicates via Bluetooth.

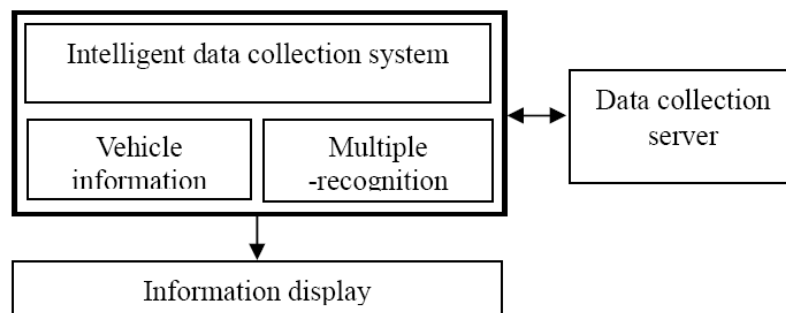


FIGURE 1. Wireless network system for intelligent car electronics

Figure 1 presents the multiple recognition system integration model for intelligent car electronics using sensors, wireless communication, a recognition system, and a mobile device for the car's transmitted information at any time. The memory device receives the car electronic data to be encoded and distributed, and the data are then transmitted to the data collection server following the GPRS model shown in Figure 2. Figure 3 shows the detection of an RFID tag combined with a video device for face recognition, which transmits the multi-recognition information to the database server center for the security system model. Figures 4 and 5 represent the end server and display the car's information and messages. The system is synchronized to send GPS data, RFID user information and messages.

3. Face Recognition. Face recognition technology can be used for a wide range of applications, such as identity authentication, access control and surveillance. Interests and research activities in face recognition have increased significantly over the past few years. A face recognition system should be able to deal with various changes in face images. Every face image in the database is represented as a vector of weights, which is the projection of the face image to a basis in eigenface space. Usually, the nearest

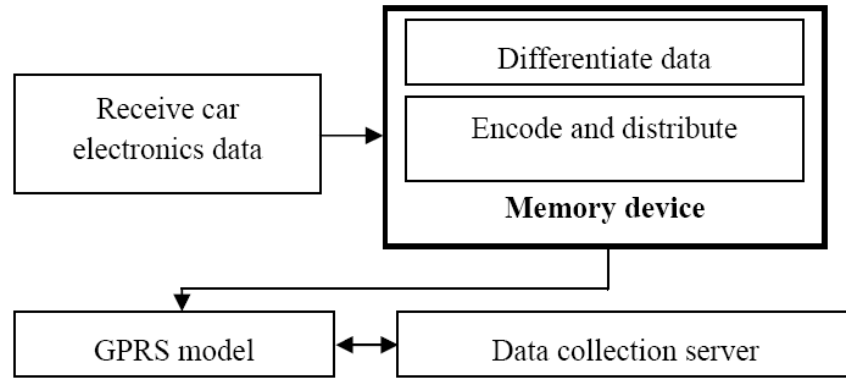


FIGURE 2. Intelligent data collection system model

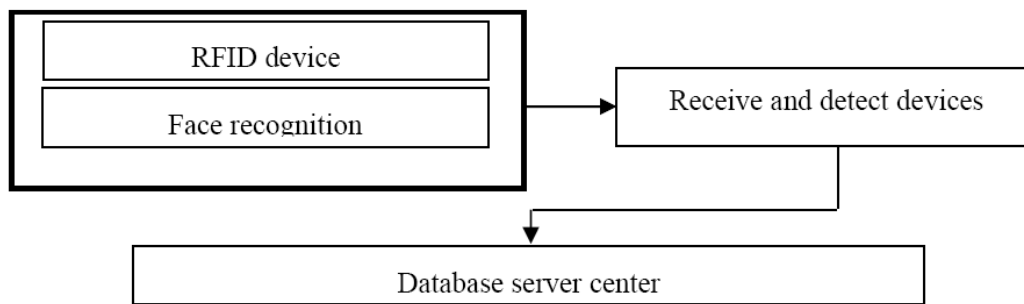


FIGURE 3. Safety care monitor system model



FIGURE 4. Intelligent data collection system program for vehicle information

distance criterion is used for face recognition [7,9]. Figure 6 presents an image with basically uniform intensity, and the difference between the average gray values of the center part and the upper round part is significant. To train the face recognizer, we first ran the component-based detector over each image in the training set and extracted the components, as shown in Figure 7.

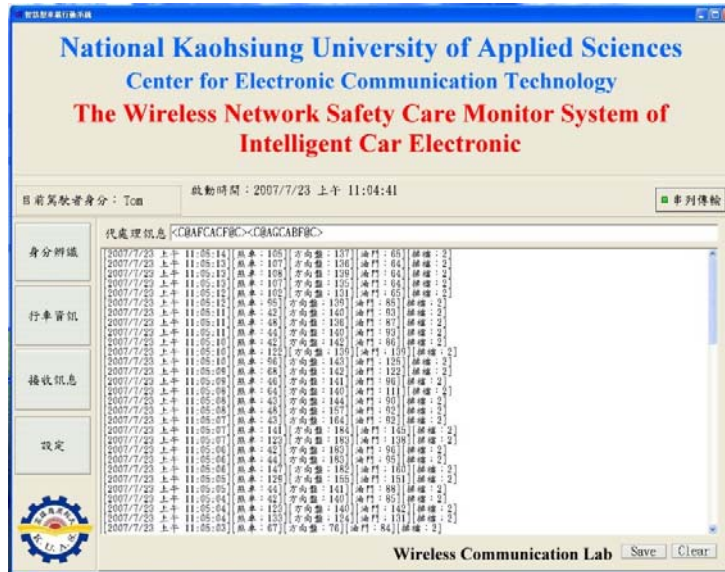


FIGURE 5. Intelligent data collection system program for received data

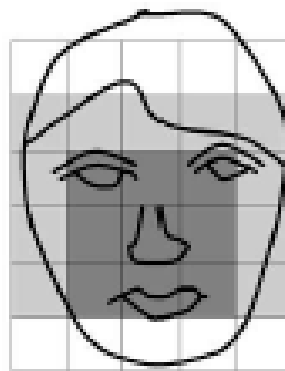


FIGURE 6. A typical face localization



FIGURE 7. (a) Image for the face detector; (b) image for face recognition

3.1. Support vector machine (SVM). We describe a system for the detection and localization of human faces in images using a support vector machine (SVM). It has been shown that SVMs provide state-of-the-art accuracy in object detection. In time-critical applications, however, they are of limited use due to their computationally expensive decision functions. In particular, the time complexity of an SVM classification operation

is characterized by two parameters. First, it is linear in the number of support vectors (SVs) used. Second, it scales with the number of operations needed for computing the similarity between an SV and the input, i.e., the complexity of the kernel function. When classifying image patches of size $h \times w$ using plain gray value features, the decision function requires an $h \cdot w$ dimensional dot product for each SV. As the patch size increases, these computations become extremely expensive. Burges introduced a method that, for a given SVM, creates a set of so-called reduced set vectors (RSVs) that approximate the decision function [8].

Intuitively, given a set of points belonging to two classes, a SVM finds the hyper plane that separates the largest possible fraction of points of the same class on the same side, while maximizing the distance from either class to the hyper plane.

Let us assume that an SVM has been successfully trained on the problem at hand. Let $\{\mathbf{X}_1, \dots, \mathbf{X}_m\}$ denote the set of SVs, $\{\alpha_1, \dots, \alpha_m\}$ the corresponding coefficients, $k(\cdot, \cdot)$ the kernel function and b the bias of the SVM solution. The decision rule for a test pattern \mathbf{X} reads:

$$f(\mathbf{X}) = \text{sgn} \left(\sum_{i=1}^m y_i \alpha_i k(\mathbf{X}_i, \mathbf{X}) + b \right) \quad (1)$$

In SVMs, the decision surface induced by f corresponds to a hyperplane in the reproducing to a kernel Hilbert space (RKHS) associated with k . The corresponding normal:

$$\Psi = \sum_{i=1}^m y_i \alpha_i k(\mathbf{X}_i, \cdot) \quad (2)$$

can be approximated using a smaller, so-called reduced set (RS) $\{\mathbf{Z}_1, \dots, \mathbf{Z}_{m'}\}$ of size $m' < m$, i.e., an approximation to Ψ of the form:

$$\Psi = \sum_{i=1}^m \beta_i k(\mathbf{Z}_i, \cdot) \quad (3)$$

This speeds up the decision process by a factor of m/m' . To find Ψ' , we fix a desired set size m' and solve:

$$\min \|\Psi - \Psi'\|_{\text{RKHS}}^2 \quad (4)$$

for β_i and \mathbf{Z}_i . Here, $\|\cdot\|$ denotes the Euclidian norm in the RKHS. The resulting RS decision function f' is then given by:

$$f'(\mathbf{X}) = \text{sgn} \left(\sum_{i=1}^m \beta_i k(\mathbf{Z}_i, \mathbf{X}) + b \right) \quad (5)$$

In practice, β_i and \mathbf{Z}_i are found using a gradient-based optimization technique [8].

A best-fit intensity plane was subtracted from the gray values to compensate for cast shadows. Then a histogram equalization was applied to remove variations in the image brightness and contrast. The resulting gray values were normalized to be in a range between 0 and 1 and were used as input features to a linear SVM classifier [9].

3.2. Linear separable filters. From the image matrix, it is obvious that the separability property can be described by a matrix rank constraint. The application of a linear filter to an image amounts to a two-dimensional convolution of the image with the impulse response of the filter. In particular, if \mathbf{I} is the input image, \mathbf{H} the impulse response, i.e., the filter mask, and \mathbf{J} the output image, then:

$$\mathbf{J} = \mathbf{I} * \mathbf{H} \quad (6)$$

If \mathbf{H} has size $h \times w$, the convolution requires $O(h \cdot w)$ operations for each output pixel. However, in special cases where \mathbf{H} can be decomposed into two column vectors \mathbf{a} and \mathbf{b} such that:

$$\mathbf{H} = \mathbf{a}\mathbf{b}^T \quad (7)$$

we can rewrite Equation (6) as:

$$\mathbf{J} = [\mathbf{I} * \mathbf{a}] * \mathbf{b}^T \quad (8)$$

because the convolution is associative and, in this case, $\mathbf{a}\mathbf{b}^T = \mathbf{a} * \mathbf{b}^T$. This splits the original Equation (6) into two convolution operations with masks of size $h \times 1$ and $1 \times w$, respectively [8]. As a result, if a linear filter is separable in the sense of Equation (7), the computational complexity of the filtering operation can be reduced from $O(h \cdot w)$ to $O(h + w)$ per pixel by computing (8) instead of (6).

3.3. Linear rank deficient filters. With Equation (7) being equivalent to $\text{rank}(\mathbf{H}) \leq 1$, we can now generalize the above concept to linear filters with low rank impulse responses. Let us consider the singular value decomposition (SVD) of the $h \times w$ matrix \mathbf{H} :

$$\mathbf{H} = \mathbf{U}\mathbf{S}\mathbf{V}^T \quad (9)$$

and recall that \mathbf{U} and \mathbf{V} are orthogonal matrices of size $h \times h$ and $w \times w$, respectively, whereas \mathbf{S} is diagonal (the diagonal entries are singular values) and has size $h \times w$. Now let $\gamma = \text{rank}(\mathbf{H})$. Because $\text{rank}(\mathbf{S}) = \text{rank}(\mathbf{H})$, we can write \mathbf{H} as a sum of γ rank-one matrices:

$$\mathbf{H} = \sum_{i=1}^{\gamma} s_i \mathbf{u}_i \mathbf{v}_i^T \quad (10)$$

where s_i denotes the i th singular value of \mathbf{H} and \mathbf{u}_i , \mathbf{v}_i are the i th columns of \mathbf{U} and \mathbf{V} (i.e., the i th singular vectors of the matrix \mathbf{H}), respectively. As a result, the corresponding linear filter can be evaluated as the weighted sum of γ separable convolutions:

$$\mathbf{J} = \sum_{i=1}^{\gamma} s_i [I * \mathbf{u}_i] * \mathbf{v}_i^T \quad (11)$$

and the computational complexity drops from $O(h \times w)$ to $O(\gamma \cdot (h + w))$ per output pixel [8].

3.4. Nonlinear rank deficient filters and reduced sets. Due to the fact that in 2D, correlation is identical to convolution if the filter mask is rotated by 180 degrees, we can apply the above idea to any image filter $f(\mathbf{X}) = g(c(\mathbf{H}, \mathbf{X}))$, where g is an arbitrary nonlinear function and $c(\mathbf{H}, \mathbf{X})$ denotes the correlation between image patches \mathbf{X} and \mathbf{H} . In SVMs, this amounts to using a kernel of the form:

$$k(\mathbf{H}, \mathbf{X}) = g(c(\mathbf{H}, \mathbf{X})) \quad (12)$$

If \mathbf{H} has rank γ , we can split the kernel evaluation into γ separable correlations plus a scalar nonlinearity. As a result, if the RSVs in a kernel expansion such as Equation (5) satisfy this constraint, the average computational complexity decreases from $O(m' \cdot h \cdot w)$ to $O(m' \cdot \gamma \cdot (h + w))$ per output pixel. This concept works for many off-the-shelf kernels used in SVMs. Although linear, polynomial and sigmoid kernels are defined as functions of input space dot products and therefore immediately satisfy Equation (12), the idea applies to kernels based on Euclidian distances as well. For instance, the Gaussian kernel reads:

$$k(\mathbf{H}, \mathbf{X}) = \exp(\gamma(c(\mathbf{X}, \mathbf{X}) - 2c(\mathbf{H}, \mathbf{X}) + c(\mathbf{H}, \mathbf{H}))) \quad (13)$$

Here, we will evaluate the middle term via separable filters. The first term is independent of the SVs; it can be efficiently pre-computed and stored in a separate image. The last

term is merely a constant scalar independent of the image data. We can use our image-matrix notation due to the fact that the squared Euclidian distance between two vectors of gray values \mathbf{x} and \mathbf{z} can be written as:

$$\|\mathbf{x} - \mathbf{z}\|^2 = \|\mathbf{X} - \mathbf{Z}\|_F^2 \quad (14)$$

Whereas the dot product amounts to:

$$\mathbf{x}^T \mathbf{z} = \frac{1}{2} (\|\mathbf{X}\|_F^2 + \|\mathbf{Z}\|_F^2 - \|\mathbf{X} - \mathbf{Z}\|_F^2) \quad (15)$$

where \mathbf{X} and \mathbf{Z} are the corresponding image patches and $\|\cdot\|_F$ is the Frobenius norm for matrices [8].

3.5. Face detection system by cascaded evaluation. At the time of detection, each pixel of an input image is the potential center of a face. To detect faces at different scales, an image pyramid is constructed. If w and h are the width and the height of the input image and L and s are the number of sub-sampling levels and the sub-sampling rate, respectively, the total number of patches to be evaluated is $N_p = \sum_{l=1}^L whs^{2(l-1)}$. Evaluation of the full SVM or even the whole set of reduced vectors on all patches would be extremely time-consuming. A large portion of the patches can be easily classified using only a few reduced-set machine algorithms using a cascaded evaluation, to be applied to each overlapping patch \mathbf{X} of an input image.

- 1) Set the hierarchy level to $j = 1$.
- 2) Evaluate:

$$y_j = \text{sgn} \left(\sum_{i=1}^j \beta_{j,i} K_i + b \right), \text{ where } K_i = k(\mathbf{Z}_i, \mathbf{X}) \quad (16)$$

- 3) If $y_j < 0$, \mathbf{X} is classified as a non-face image, and the algorithm stops.
If $y_j \geq 0$, j is incremented. If $j < N_Z$, the algorithm continues from step (2).
If $j = N_Z$, it continues from step (4).
- 4) When this step is reached, $y_j \geq 0$ and $j = N_Z$, the full SVM is applied on the patch \mathbf{X} , using Equation (1). If the evaluation is positive, the patch is classified as a face.

The main feature of this approach is that, on average, very few kernels K_i have to be evaluated at any given image location, i.e., for most patches, the algorithm above stops at a level $j \ll N_Z$. This speeds up the algorithm relative to the full reduced set. A substantial speed-up can be obtained not only for the face-detection problem but for any classification application for which the number of instances of the two classes to be evaluated is highly asymmetric, as is the case for face detection (where most of the patches do not depict a face). Note that, in the case of Gaussian kernels, the application of one reduced-set vector amounts to a simple template-matching operation [10].

The geometrical configuration classifier performed the final face detection by combining the results of the component classifiers. The search regions calculated from the mean and standard deviation of the components' locations in the training images are shown in Figure 8. Detection and recognition simulation of the driver's face in light and at night in a car are shown in Figures 9 and 10.

4. RFID Technology. RFID stands for radio frequency identification. It is an automatic identification technology whereby digital data encoded in a RFID tag or smart label are captured by a reader using radio waves. It uses a mobile phone as an RFID reader with wireless technology and provides new valuable services to users by integrating RFID and wireless mesh network infrastructure with mobile communication and wireless Internet [12].

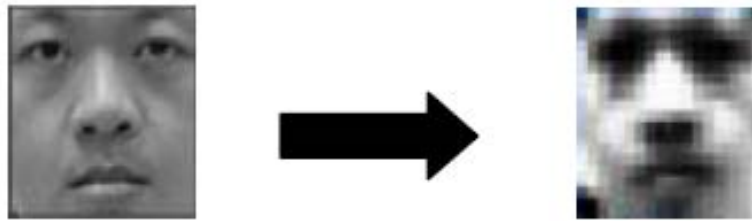


FIGURE 8. Detection of components



FIGURE 9. Face dynamical detection and recognition



FIGURE 10. Simulated face detection and recognition for a car

RFID systems using a contact-less IC card or IC tag are used as automatic ticket checkers in railway stations, as security systems checking people entering or exiting buildings, and in electronic money systems. New fabrication techniques and algorithms providing better security have been developed such that mobile systems using RFID communication systems are now possible. An electromagnetic field radiating from a loop antenna provided in the reader/writer is coupled by electromagnetic induction to a loop antenna in the IC card. However, if the loop antenna is installed on metallic housing such as that of a PDA (personal digital assistant) or a mobile phone, the loop antenna for the reader/writer cannot efficiently radiate an electromagnetic field to the IC card: due to eddy current loss, the communication range between the IC card and the reader/writer

is narrow. Current non-portable products apply magnetic sheets to minimize the influence of metallic housing; however, a small, thin magnetic sheet for mobile systems is not effective in allowing communication with a reader/writer at some distance [13], as shown as Figure 11.



FIGURE 11. RFID chip model

4.1. RFID security. Encrypting a tag identifier may seem to be a good solution for addressing the problems of privacy, but it does not solve all problems because an encrypted identifier is itself just another identifier. There have been an increasing number of studies related to encryption, but it would be difficult to apply them to low-cost tags because of this problem [12].

This problem is similar to that of wireless LANs. Normally, a WLAN is only effective for a user within 100 m or so. For instance, if an RFID tag is designed to be read at 1 ft, an attacker may still be able to interact with it at 100 ft away. RFID tags typically only contain a unique number that is useless on its own. The idea is that the reader interfaces with some backend system and database for all transactions. The database stores information that ties the unique ID to something of interest. For instance, the database knows that ID 1234 is attached to a bar of soap. An attacker reading RFIDs would not know, without access to the database, what ID 1234 refers to.

The vast majority of RFID tags on the market require no authentication for reading their information. This allows anyone, an attacker or even simply a competitor, to read the data on an RFID chip. Furthermore, many tags have the capability to write information to the chip without authentication. This is especially troubling for enterprises relying on RFID for things like supply chain management. An attacker could theoretically overwrite values on RFID tags used by the enterprise, thereby wreaking havoc with their RFID system [14].

5. The Wireless GPRS Model Network for Traffic. With the evolution of mobile technologies and increased user demands, the market of mobile communication has grown rapidly in recent years. It is clear that the traditional voice services no longer satisfy mobile users. Like any other packet data service, the aim of GPRS is to dynamically share physical resources with users and efficiently accommodate burst data sources. The physical layer of the GSM system uses a time division multiple access (TDMA) frame structure. The basic resource unit is a time slot (TS) without sharing between multiple

voice sources, unlike the voice transmission in GSM, although the GPRS system shares the same TDMA frame structure [15].

Air Interface Dimensioning: To determine the required GPRS, the interface capacity is an estimate of the amount of data traffic that a given call will be required to handle in a busy hour because voice transmission occurs in real time, whereas data transmission does not. The RF capacity of a given GPRS based on the number of GPRS users in a cell can be calculated. The advantage of GPRS is its use of packet-switching technology. It enables multiple users to share air interface resources for the GSM/GPRS model of a car black box, as shown as Figure 12. Because this is a request-allocation procedure, the users feel that their services are “always on” [16].



FIGURE 12. The GSM/GPRS model of a car black box

5.1. The GSM/GPRS model. A GSM/GPRS cell can be modeled as a loss system with total capacity C , offered a finite number k of traffic streams, each describing a different service. Depending on the partitioning strategy, C is divided into, at most, three partitions: C_{GSM} , the capacity used exclusively for traditional GSM voice calls, C_{GPRS} , the capacity used exclusively for GPRS, and C_{Common} , the capacity shared by all services. The total cell capacity of the system C depends on the actual number of frequencies used in the cell.

Let $X_i(t)$ denote the number of calls of type i in progress in the system at time t . $\mathbf{X}(t) = (X_1(t), \dots, X_k(t))$ defines a continuous-time stochastic process with finite discrete state space. The set of allowed states Ω depends on the admission policy, to be defined later. Assuming that the process $\mathbf{X}(t)$ reaches a steady state for $t \rightarrow \infty$, let $p(\mathbf{x})$, $\mathbf{x} = (x_1, \dots, x_k)$, $\mathbf{x} \in \Omega$ be the steady-state probabilities.

The vector $\mathbf{b}(\mathbf{x}) = (b_1(\mathbf{x}), \dots, b_k(\mathbf{x}))$, $\mathbf{x} \in \Omega$ defines the individual state-dependent bit rates, where $b_i(\mathbf{x})$ is the bit rate of one type i call in state \mathbf{x} . It is assumed that calls of the same type transmit with the same bit rate somewhere between 0 and $b_i^{(\max)}$. This behavior can be achieved by the base station because it has complete control over the

capacity of the system in up- and downlinking. With the limitation that a mobile station (MS) can receive only one frequency at a time, $b_i^{(\max)}$ will not be greater than C_f , where C_f is the maximum capacity of one frequency. To introduce as much flexibility as possible into the bit rate allocation, a *bit rate threshold vector* $b_i^{(\min)}$, $\min = (\min_1, \dots, \min_k)$ is assigned to each service type i . The threshold $b_i^{(\min_j)}$ is called the *minimum occupied bit rate* of a call of type i with respect to calls of type j and is the minimum bit rate that calls of type i have to reduce to in favor of the arrival of type j calls. A value of $b_i^{(\min_j)} = 0$ means that an arrival of a type j call can cause a disruption of an ongoing type i call. A *softly occupied bit rate* of a call of type i with respect to calls of type j in state \mathbf{x} is defined as the difference $b_i(\mathbf{x}) - b_i^{(\min_j)}$. This difference is the capacity that can be released immediately. The values of the *bit rate threshold vector* satisfy the condition $0 \leq b_i^{(\min_j)} \leq b_i^{(\max)}$, $j = 1, \dots, k$.

The parameters $C_i^{(n)}$ and $C_i^{(ho)}$ representing new calls and handover calls, respectively, are introduced. They are called *capacity reservation thresholds*. A partition in which calls of type i can be admitted is called an i -partition. Then $C_i^{(n)}$ ($C_i^{(ho)}$) is the maximum value for the sum of the *minimum occupied bit rates* of all services in all i -partitions, after the acceptance of a new handover type i call. In the following, $C_i^{(n)} < C_i^{(ho)}$ will be assumed, so handover arrivals will always be treated with priority over new arrivals.

Let the voice service be the only service in the GSM partition, denote it by $i = 1$ and denote the GPRS services by $i = 2, \dots, k$. To use the whole system capacity, the following conditions must hold [17].

- 1) Complete partitioning (CP) divides the total cell capacity into two parts, one for GSM and one for GPRS traffic. At the early introduction phase, little capacity should be dedicated to GPRS traffic due to the low penetration of GPRS terminals.

$$C_{GSM} = C_1^{(ho)} \text{ and } C_{GPRS} = \max \left(C_2^{(ho)}, \dots, C_k^{(ho)} \right) \quad (17)$$

- 2) Complete sharing (CS) does not exclusively assign capacities to GSM or GPRS traffic. Only for incoming handovers is capacity reserved. Therefore, this strategy promises the lowest influence of the introduction of GPRS on traditional GSM service.

$$C_{GPRS} = \max \left(C_1^{(ho)}, \dots, C_k^{(ho)} \right) \quad (18)$$

- 3) Partial sharing (PS) divides the total cell capacity into three parts, one for GSM, one for GPRS traffic and one common partition. The GPRS partition has to be large enough to guarantee a certain QoS and small enough that no bandwidth is wasted in the case of very low GPRS traffic.

$$\begin{aligned} C_{GSM} + C_{Common} &= C_1^{(ho)} \\ C_{GPRS} + C_{Common} &= \max \left(C_2^{(ho)}, \dots, C_k^{(ho)} \right) \end{aligned} \quad (19)$$

In the following, an admission policy is introduced that can reserve capacity for high-priority calls (e.g., handover voice calls), while maintaining a high utilization of the partition resources. The main idea is to utilize the reserved capacity by a softly occupied bit rate that can be released immediately upon request. In state \mathbf{x} , a new arrival of type i is accepted, if, after its admission, the sum of the minimum occupied bit rates of all services in all i -partitions is not greater than $C_i^{(n)}$. Depending on the admission policy, the following conditions must hold:

- 1) CP:

$$x_1 b_1^{(\min_1)} \leq C_1^{(n)} - b_1^{(\min_1)} \text{ (GSM),}$$

$$\sum_{j=2}^k x_j b_j^{(\min_i)} \leq C_i^{(n)} - b_i^{(\min_i)}, \quad i = 2, \dots, k \text{ (GPRS)}. \tag{20}$$

2) CS:

$$\sum_{j=2}^k x_j b_j^{(\min_i)} \leq C_i^{(n)} - b_i^{(\min_i)}, \quad i = 1, \dots, k \text{ (GSM, GPRS)}. \tag{21}$$

3) PS:

$$\begin{aligned} &\sum_{j=1}^k x_j b_j^{(\min_1)} - C_{GPRS} \leq C_1^{(n)} - b_1^{(\min_1)}, \\ x_1 b_1^{(\min_1)} &\leq C_1^{(n)} - b_1^{(\min_1)} \text{ (GSM)}, \quad \sum_{j=1}^k x_j b_j^{(\min_i)} - C_{GSM} \leq C_i^{(n)} - b_i^{(\min_i)}, \\ &\sum_{j=2}^k x_j b_j^{(\min_i)} \leq C_i^{(n)} - b_i^{(\min_i)}, \quad i = 2, \dots, k \text{ (GPRS)}. \end{aligned} \tag{22}$$

For handover arrivals, the same admission conditions apply, except that the *capacity reservation threshold* for handover $C_i^{(ho)}$ is used, instead of $C_i^{(n)}$. There are different approaches to distributing the capacity of the system among calls. As mentioned above, calls of the same type always transmit with the same bit rate. Let us assume that the services are ordered according to their priorities in descending order, with voice calls having the highest priority and a state-independent constant bit rate [14]. Then the bit rate of one type i GPRS call in state \mathbf{x} is set to:

$$\begin{aligned} b_i(\mathbf{x}) &= \min \left(\max(b_A, b_i^{(\min)}), b_i^{(\max)} \right), \quad i = 2, \dots, k, \\ b_A &= (C^* - \sum_{j=2}^{i-1} x_j b_j^{(\max)} - \sum_{j=i+1}^k x_j b_j^{(\min)}) / x_i, \\ b_j^{(\min)} &= \min \left(b_j^{(\min_1)}, \dots, b_j^{(\min_k)} \right), \end{aligned} \tag{23}$$

and

$$C^* = \begin{cases} C_{GPRS} & \text{for CP,} \\ C - x_1 b_1^{(\max)} & \text{for CS,} \\ C_{GPRS} + C_{Common}, x_1 b_1^{(\max)} \leq C_{GSM} & \text{for PS,} \\ C - x_1 b_1^{(\max)}, x_1 b_1^{(\max)} > C_{GSM} & \text{for PS.} \end{cases} \tag{24}$$

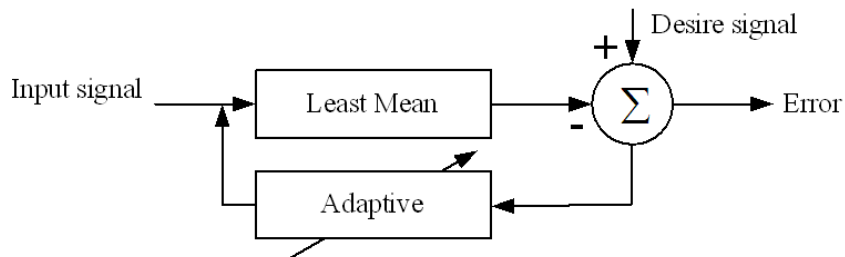


FIGURE 13. Adaptive LMS analysis model for V2I transmission

We proposed an adaptive V2I heterogeneous communication model in vehicular networks. Through the adaptive least mean square (LMS) analyze module, we can realize relation between the mean square error and the number of hops, As Figure 13, we consider

two paths without correlations as shown Figure 14. For the case without correlations, Figure 14 shows the mean square error with respect to the number of hops, with the Poisson packet arrivals, while the tow-hop two-path estimator of the deterministic packet arrival is a lower bound benchmark due to inherent deterministic information in each time slot.

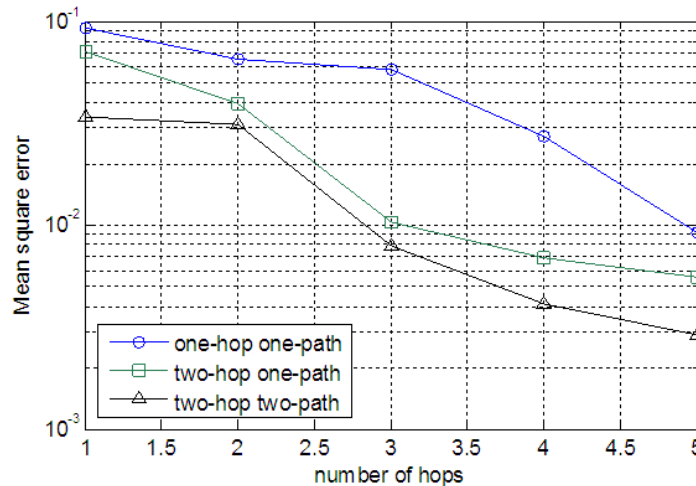


FIGURE 14. Number of hops with MSE

6. Conclusions. In recent years, the government has managed traffic issues with scientific data to investigate and handle car incidents. Therefore, the car black box should play a very important role. In this work, a car black box system was integrated with RFID and face recognition, so that the system can confirm the driver's identity and connect to a safety system. The black box system includes a GPS device adopted to monitor the car's speed, direction, static state and dynamic state at any time. In addition, it can prevent vehicles from being stolen. The car black box is an applied management system of transport service.

This system organizes modernization with the idea of "machine replaces manpower" as the rationalized foundation. It promotes traffic safety and the management operation for systematization and rationalization. The car black box can also include a camera on the rearview mirror; it could record images and sounds within the car.

REFERENCES

- [1] S. Biswas, R. Tatchikou and F. Dion, Vehicle-to-vehicle wireless communication protocols for enhancing highway traffic safety, *IEEE Comm. Magazine*, vol.44, no.1, pp.74-82, 2006.
- [2] L. Yang and F.-Y. Wang, Driving into intelligent spaces with pervasive communications, *IEEE Intelligent Systems*, vol.22, no.1, pp.12-15, 2007.
- [3] W. D. Jones, Black boxes get green light car crash data recorders, *IEEE Spectrum*, vol.41, no.12, pp.14-16, 2004.
- [4] L. Ljung, Black-box models from input-output measurements, *Proc. of the 18th IEEE Instrumentation and Measurement Technology Conference*, vol.1, pp.138-146, 2001.
- [5] Z. Zhu, X. Chen, F. Zhang and J. Sui, Study on data fusion method in geographic information system for transportation, *IEEE Int. Geoscience and Remote Sensing Symposium*, vol.2, pp.4, 2005.
- [6] J. Jin, Z. Qiu and B. Ran, Intelligent route-based speed estimation using timing advance, *IEEE Intell. Transp. Systems*, pp.194-197, 2006.
- [7] G. Guo, S. Z. Li and K. Chan, Face recognition by support vector machines, *Proc. of the IEEE Int. Conf. Automatic Face and Gesture Recognition*, pp.196-201, 2000.

- [8] W. Kienzle, G. Bakir, M. Franz and B. Schölkopf, Face detection-efficient and rank deficient, in *Advances in Neural Information Processing Systems 17*, L. K. Saul, Y. Weiss and L. Bottou (eds.), USA, MIT Press, 2005.
- [9] B. Heisele, P. Ho and T. Poggio, Face recognition with support vector machines: Global versus component-based approach, *Proc. of the 8th IEEE Int. Conf. on Computer Vision*, vol.2, pp.688-694, 2001.
- [10] S. Romdhani, P. Torr, B. Schölkopf and A. Blake, Efficient face detection by a cascaded support-vector machine expansion, *Proc. of the Royal Society A: Mathematical, Physical and Engineering Sciences*, vol.460, no.2051, 2004.
- [11] M.-H. Yang, D. J. Kriegman and N. Ahuja, Detecting faces in images: A survey, *IEEE Trans. on Pattern Analysis and Machine Intelligence*, vol.24, no.1, pp.34-58, 2002.
- [12] H. Lee and J. Kim, Privacy threats and issues in mobile RFID, *availability, reliability and security*, pp.5, 2006.
- [13] H. Ryoson, K. Goto, M. Ueno, A. Kikuchi and Y. Shimpuku, A 13.56 MHz RFID device and software for mobile systems, *IEEE Consumer Comm. and Networking Conference*, pp.241-244, 2005.
- [14] B. Potter, RFID: Misunderstood or untrustworthy? *Network Security*, vol.1, no.4, pp.17-18, 2005.
- [15] C.-N. Tsai, Sharing and multiplexing of downlink traffic resources in mobile packet data networks, *Parallel and Distributed Systems*, vol.1, pp.523-529, 2005.
- [16] W. C. Y. Lee, *Wireless and Cellular Telecommunications*, McGraw-Hill, Inc, 2005.
- [17] M. Ermel, T. Müller, J. Schüler, M. Schweigel and K. Begain, Performance of GSM networks with general packet radio services, *Performance Evaluation*, vol.48, no.1-4, pp.285-310, 2002.
- [18] I.-S. Hwang, B.-J. Hwang and L.-F. KU, Heterogeneous wireless networks, *Journal of Computer Sciences and Engineering Systems*, vol.3, no.2, 2009.
- [19] Z. Wang, Q. Han, C. Busch and X. Niu, A secure face recognition system, *Journal of Computer Sciences and Engineering Systems*, vol.3, no.2, 2009.
- [20] M. K. J. Kumar and R. S. Rajesh, Distributed positioning technique in wireless ad hoc sensor networks, *Journal of Computer Sciences and Engineering Systems*, vol.2, no.3, pp.193-199, 2008.
- [21] Z.-G. Zhu, H.-K. Xiang, J.-W. Liu, Q. Cao and T. Yu, Research on traffic data-collecting system based on MC9S12D64 microcontroller, *Journal of Computer Sciences and Engineering Systems*, vol.1, no.1, pp.1-6, 2007.
- [22] A. Habbani, O. Romain and P. Garda, MIS and I2C bus, *Journal of Computer Sciences and Engineering Systems*, vol.1, no.2, pp.111-117, 2007.
- [23] H. Kurihata, T. Takahashi, I. Ide, Y. Mekada, H. Murase, Y. Tamatsu and T. Miyahara, Detection of raindrops on a windshield from an in-vehicle video camera, *International Journal of Innovative Computing, Information and Control*, vol.3, no.6(B), pp.1583-1591, 2007.
- [24] K. Mori, T. Takahashi, I. Ide, H. Murase, T. Miyahara and Y. Tamatsu, Fog density recognition by in-vehicle camera and millimeter wave radar, *International Journal of Innovative Computing, Information and Control*, vol.3, no.5, pp.1173-1182, 2007.